Hydrogen-bond network distortion of water in the soft confinement of Nafion membrane

M. Plazanet, I. Morfin, V. Honkimäki, T. Buslaps, C. Petrillo, F. Sacchetti

Hydrogen-bond network distortion of water in the soft confinement of Nafion membrane.

M. Plazanet,[1, a)] I. Morfin,[1] V. Honkimäki,[2] T. Buslaps,[2] C. Petrillo,[3] and F. Sacchetti[3]

[1)] *LIPhy, University Grenoble-Alpes and CNRS UMR5588*[b)]

[2)] *ESRF, F-38042 Grenoble, France*

[3)] *Dipartimento di Fisica e Geologia, Università degli Studi di Perugia, I-06123 Perugia, Italy*

(Dated: 1 June 2021)

A Compton spectroscopy investigation is carried out in hydrated Nafion membranes enabling to identify distortions in the hydrogen bond distribution of the polymer hydrating water, by means of the subtle changes reflected by the Compton profiles. Indeed, deformations of the Compton profiles are observed when varying hydration and two different bonding kinds are associated to the water molecules: at low hydration, water surrounds the sulfonic groups while, on increasing hydration, water molecules occupy the interstitial cavities formed upon swelling of the membrane. The analysis is proposed in terms of averaged OH bond length variation. A sizable contraction of the OH distance is observed at low hydration (~ 0.09 Å), while at higher hydration levels the contraction is smaller (~ 0.02 Å) and the OH bond length is closer to bulk water. An evaluation of the electron kinetic energy indicates that the spatial changes associated to the water distribution correspond to a consistent binding energy increase. Distinct temperature dependences of each water population are observed, which can be straightly related to water desorption into ice on cooling below the freezing point.

[a)] Electronic mail: marie.plazanet@univ-grenoble-alpes.fr

[b)] Also at Dipartimento di Fisica, Università degli Studi di Perugia, I-06123 Perugia, Italy

INTRODUCTION

Interstitial, hydration or confined water is present in a countless number of systems, in particular in soft and deformable media whose properties are finely tuned by their water content. The confinment of water to different length scales down to nanometer is very important in a wide range of systems for both basic science and applications[1]. Swelling of polymers is an interesting example of water that enters the material occupying a large number of sites, as isolated molecules nearly bound to the matrix (through e.g. hydrogen bonding), or forming nano-droplets. Hydration often causes release of acidic protons, then freely diffusing inside the matrix. An archetypal material with such properties is Nafion®, used as Polymer Exchange Membrane for fuel cells thanks to the diffusion of hydronium ions that enable proton conductivity across the membrane[2,3]. Nafion is an amphiphilic polymer with fluorinated backbone and sulfonic terminations, where hydrogen bonds are present. These hydrophilic groups are organized to form a percolating network of channels or cavities, with dimensions up to a few nanometers[4–6]. Nafion suffers strong swelling, with water entering and enlarging the cavities network but also deforming the polymeric matrix, in particular when soaked into water[7,8].

As known, confined water properties such as melting point, relaxation times or vibrational characteristics[9–11], differ from bulk counterpart. Nonetheless, the effects of fine structural organization on these properties is hardly investigated in the liquid state, because of the instrumental limitations of most experimental techniques. Confined water properties, like for example the density, are often deduced from measurements of the hydrated matrix assuming structural characteristics of the matrix as known and a homogeneous filling of the volume fraction occupied by water[12]. Because of the size heterogeneities of the cavities, the roughness of the surfaces etc., this picture may be far from reality, as it was already pointed out[12].

In this context, X-ray Compton spectroscopy[13] is an extremely high sensitivity probe of the molecular structure through the momentum distribution of valence electron states, which are responsible for molecular bonding, differently from X-ray diffraction where the signal is dominated by core electrons. Compton spectroscopy is sensible to subtle bonding effects like those expected in confined water and the data interpretation does not contain strong assumptions on the structure or guesses on the volume fraction occupied by water.

In cases where the matrix contribution is unchanged under hydration, measured observables like the electron momentum density and the kinetic energy are related to water properties only. On the other hand, for rather strong swelling the electron distribution of the matrix is also affected and a careful separation of the contributions has to be applied, as we discuss in the following sections.

To investigate confined water arrangements in a Nafion membrane, we present in this paper a temperature dependent Compton spectroscopy study on samples at various hydration levels. A careful analysis of the so-called Compton profile (CP)[13], which is directly determined in a Compton spectroscopy experiment, enables to identify the structural variations of the system in different swelling conditions. Our analysis reveals a deformation of the average OH bond length of the confined water as determined from the Compton profile using a simple empiric procedure derived from model calculations[14]. A deformation of the matrix is simultaneously observed upon swelling. As a consequence, on increasing the hydration level, one is facing the presence of different components in a single sample, namely original *dry nafion matrix* (dm), the *modified nafion membrane* when affected by the hydration water, *confined water* (cw) in two different conditions, that is *strongly bonded water* present when the water is bonded to the sulfonic group, and *weakly bonded water* found as interstitial water producing appreciable swelling of the membrane. The temperature dependence shows that the hydrogen bond network distortion increases at lower temperature. The kinetic energy of water consistently increases when the molecule interacts with the membrane, enabling the distinctions of the two water populations, i.e. bound and interstitial. Eventually, we propose and validate an alternative analysis of the CP based on a fit and residuals with simple atomic profiles.

I. MATERIAL AND METHODS

A. Samples

Nafion 112 was bought from Ion Power Inc. The membranes have an equivalent weight of 1100 (g membrane/mol sulfonic groups), and a thickness of 54 μm. The membranes were first cut into 10 mm diameter pieces, and then treated according to the outlined procedure. Impurities were removed by boiling the sample into 3 % hydrogen peroxide solution and

rinsed with deionized water. To remove all the eventual cations (K^+, Na^+) occupying the SO_3^- sites, the membranes were boiled into 0.5M H_2SO_4 for one hour and rinsed again. The sample was then sonicated for two hours in a 50% ethanol solution to remove small polymers and fragments remaining from the synthesis. Eventually, it was boiled three times for one hour in H_2O[15,16].

The fully hydrated membranes were boiled in H_2O for 15 minutes and immediately placed and closed into the cell for the Compton spectroscopy experiment, which was a sample holder made of an aluminum alloy frame with thin (0.01 mm) mylar windows to minimize scattering and absorption of the incoming and outgoing X-ray beam. By weighting the sample, it was found that the fully hydrated membrane contained $0.5\,\mathrm{g}\ H_2O/g$ of dry membrane, corresponding to about 30 molecules of water per sulfonic group. This is more than previously obtained in several works (e.g. $0.22\,\mathrm{g/g}$[17] or $0.36\,\mathrm{g/g}$,[15]). However, as we will see in the next sections, no bulk water is observed in the sample. Therefore the excess of water could be explained by a different treatment of the membrane or the higher temperature at which it was hydrated.

Lower hydration samples were produced by pumping the water out. After a long enough pumping duration ($\geq$ 10 hours), the dry state was reached. In this way, all the water but 1 molecule per sulfonic group is removed[15,18], which corresponds to $0.016\,g\,H_2O/g$ of dry membrane. The experimental error affecting the measurements did not allow to achieve a precision better than $\pm 0.01\,\mathrm{g}\,H_2O/\mathrm{g}$ of dry membrane.

To obtain a sample of sufficient thickness for the measurements, several layers were lied and squeezed between mylar windows. Two distinct samples were produced this way, containing respectively 35 and 60 layers. The first sample was left open for several days in order for it to equilibrate with ambient humidity, reaching a room hydration of $\lambda_1 = 13$ molecules of water per sulfonic group. After the Compton measurement, this sample was placed under vacuum to produce the dry sample for the experiment. The second sample was sealed right after boiling in order to reach the maximum hydration, pointing at $\lambda_4 = 65$. It was then shortly placed under vacuum to obtain an first intermediate hydration of $\lambda_3 = 49$, and further dried to reach a second intermediate hydration of $\lambda_2 = 33$. Since the polymer itself is known to deform with temperature and under swelling in a slow reversible way[7,19,20], we expect it to be identical in the dry and λ_1 sample, that was left at room temperature, but different in the $\lambda_{2,3,4}$ samples where water was forced to penetrate into the polymer at

Sample designation	nominal hydration	fitted hydration	T measured	Z
Dry matrix (dm)		—	200, 240, 258, 273, 290	532.8
$\boldsymbol{\lambda_1}$	13.7± 1.1	13.2 ± 0.8	200, 240, 258, 273, 290	662.8
$\boldsymbol{\lambda_2}$	33.0 ± 2.0	25.5 ± 0.7	200, 240, 258, 273, 290	872.8
$\boldsymbol{\lambda_3}$	49.0 ± 3.5	40.3 ± 0.7	290	1042.8
$\boldsymbol{\lambda_4}$	65.0 ± 3.5	48.3 ± 0.8	200, 240, 258, 273, 290	1182.8
Bulk water (bw)			258, 273, 290	10

TABLE I. Overview of the samples and temperature settings of the CP experiment. The nominal hydration, obtained by weighting the samples, is reported and the hydrated samples are named in the order λ_1, λ_2, λ_3 and λ_4. The hydration values deduced from the fitting procedure (see text) are also reported and further used for sample denomination. Discrepancies at high hydration levels may arise from droplets of bulk water on the side of the sample. Z are the normalization factors, equal to the number of electrons in the molecular unit of each sample (see text).

100^oC.

Measurements on bulk water were carried out using the same cell with the samples, which amounted to a thickness of 5 mm. An overview of all the samples, including the hydration data and the temperature values of the Compton measurements, is given in Table I.

B. Methods

Measurements were carried out on the ID31 beamline at the ESRF (Grenoble, FR), which is equipped with a specially designed section for the measurements of Compton profile. The sample was illuminated by a high intensity high energy monochromatic photon beam at 70 keV and the photons scattered at high angles were detected by means of a 12-element Ge solid state detector. In this configuration a good momentum resolution of $\Delta q \simeq 0.7$ a.u. was obtained. Within of the so called impulse approximation (IP)[13], the detected photon flux dN, for an incoming photon current density j_0, is written as[21]

$$dN = j_0 \frac{d^2\sigma}{d\Omega d\epsilon} d\Omega d\epsilon \tag{1}$$

where the differential cross section is given by:

$$\frac{d^2\sigma}{d\Omega d\epsilon} = r_0^2 |\mathbf{e} \cdot \mathbf{e}_0|^2 \frac{k}{k_0} \frac{J(q)}{Q} \tag{2}$$

In the above equation k_0, k, $\mathbf{e}_0$ and $\mathbf{e}$ are the incoming and outgoing photon wave vectors and polarization vectors respectively, $\mathbf{Q}$ is the momentum transfer and q is the electron momentum along the direction of $\mathbf{Q}$. The Compton profile $J(q)$ is a proper projection of the electron momentum density $n(p)$ that is assumed to be isotropic as appropriate to the present experiment:

$$J(q) = 2\pi \int_{|q|}^{+\infty} n(p)\, p \;\; dp \tag{3}$$

Note that the total integral of the Compton profile $J(q)$ equals the number of electrons per molecular unit, Z. This condition has been used to normalize the data on a common absolute scale, which is useful to compare different samples.

The membranes were mounted with the plane perpendicular to the beam axis and Compton spectra were recorded around the angle of 158^o. The sample temperature was controlled by an Oxford closed cycle cryostat operated under helium flux. Each spectrum was collected in approximately 4 hours counting.

The raw data were corrected for self absorption and multiple scattering[22], and then symmetrized around $q = 0$ for a better presentation of the data. We checked that the normalization procedure did not induced deviations larger than 1% from the unsymmetrized profiles. Finally the data were normalized to the total number of electrons in each sample.

Typical processed and normalized spectra of all the Nafion samples and the bulk water at $T = 290$ K are shown in figure 1 where the statistical errors are negligible due to the extremely high collected counts. The spectra are characterized by a rather sharp peak around $q = 0$, which is related to the valence electron states, while the broad distribution of the profile is produced by the core states. Core states are strongly bound to atomic sites being thus independent of the interatomic chemical bonding and the temperature; therefore they were assumed as independent of the atomic composition of the sample, perfectly canceling during further subtractions and not providing any contribution to the difference profiles. For

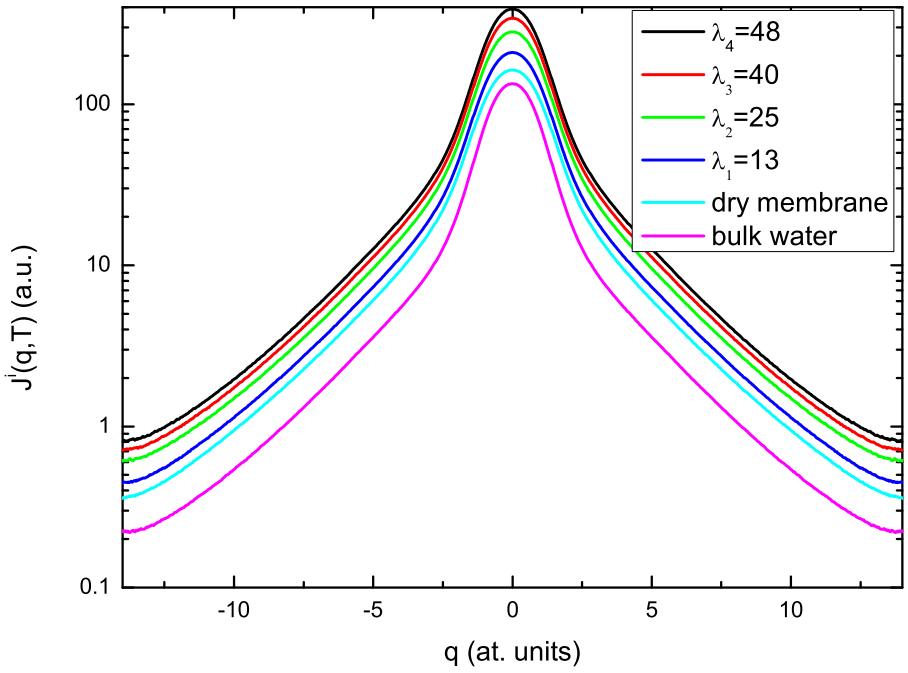

FIG. 1. Compton profile $J^i(q,T)$ at $T = 290$ K of the various λ_i samples, properly normalized after data correction (see methods). The bulk water spectrum is multiplied by 37.5 for a better comparison.

further analysis of the confined water characteristics, the dry membrame CP $J_{dm}(q,T)$ was subtracted from the hydrated Nafion CP in order to get the confined water CP: $J_{cw}(q,T) = J^i(q,T) - J_{dm}(q,T)$.

C. Analysis

In view of the complexity of this system, as sketched before, two distinct analysis are proposed in this paper. The first one relies on direct analysis of the subtraction of CP between confined water and bulk water and an examination of the differences directly in the q-spaced, compared with simulations of equivalent CP differences with DFT-based numerical modeling of water.

The second analysis returns to the real space. The Fourier transform of the CP, $B(r)$, provides information on the electron distribution in real space. In general, the Fourier transform of the momentum density distribution $n(\mathbf{p})$ gives the so called *reciprocal form factor*[13] $B(\mathbf{r})$, i.e. (in Rydberg units)

$$B(\mathbf{r}) = \int n(\mathbf{p})\, \exp(i\mathbf{p}\cdot\mathbf{r})\, d\mathbf{p} = 4\pi \int_0^\infty n(p) \frac{\sin(p\, r)\, p}{r}\, dp \tag{4}$$

where the last expression on the right hand side of the above relationship applies to isotropic systems, like the present one, where $\frac{dJ(p)}{dp} = 2\pi n(p)p$. Therefore, one has:

$$B(r) = 2 \int_0^\infty J(p) \cos(pr)\, dp \tag{5}$$

In addition, the total kinetic energy T_e of the Z electrons in the sample can be obtained from $J(p)$, as

$$T_e = 6 \int_0^\infty J(p)\, p^2\, dp \tag{6}$$

Thanks to the Virial theorem, $T_e = -E_e = -V_e/2$, E_e and V_e being the total and the potential energies. Therefore, a comparison of kinetic energies amounts to compare the binding energies, which, when applied to the present system, could enable to infer the change in the binding energy as a function of both hydration and temperature.

However, the direct determination of T_e from the experimental data suffers of termination errors in the calculation of the integrals, due to the long tails of the CPs caused by core contributions and possible systematic experimental errors. For instance, in the case of bulk water, one has $J(0) = 3.573 \pm 0.001$ a.u. and a constant *background* contribution as small as 0.0005 a.u. introduces a systematic error of about 3 Ryd (that is more than 40 eV). Therefore an absolute energy determination is extremely difficult while an internal comparison as a function of temperature is much more accurate. The same causes also strongly affects the determination of $B(r)$.

We therefore propose an alternative procedure, in extracting the part of CPs more directly related to the change of the valence electrons contribution, as a function of hydration and temperature. We performed a preliminary evaluation of the evolution of both bulk $J_{bw}(q,T)$ and confined $J_{cw}(q,T)$ water CPs, by fitting a simplistic analytic model $J^{mod}_{bw,cw}(q,T) = w_{val}(T)\, J_{val}(q) + w_{core}(T)\, J_{core}(q)$, $J_{val}(q)$ and $J_{core}(q)$ being valence and core states contributions described by analytic hydrogen-like functions. The core contribution was determined from the Oxygen 1s atom data[23] while $J_{val}(q) = 8b^5_{val}/[3\pi(q^2 + b^2_{val})^3]$, according to[21], was determined by leaving b_{val} as a free parameter together with the two weights $w_{val}(T)$ and $w_{core}(T)$. We note that b_{val} has an exact definition in the case of a single

electron, but not in such a complex system. The model, convoluted to a Gaussian shaped resolution function with 0.7 a.u. FWHM, produced a good fit of all data but a small, although not negligible, residual contribution $\Delta J^{mod}_{bw,cw}(q,T) = J_{bw,cw}(q,T) - J^{mod}_{bw,cw}(q,T)$ which is attributed to the water binding. Note that this residual is therefore similarly determined for bulk and confined water, and mainly accounts for the deviations between atoms being localized or involved in hydrogen bonds.

A typical result for the residual contribution is shown in figure 2 (left panel) where $\Delta J^{mod}_{bw}(q,T)$ and $\Delta J^{mod}_{cw}(q,T)$, respectively for bulk water and $\lambda_2 = 25$ (fitted hydration), show characteristic oscillatory trends centered around $q = 0$. Similar results are obtained for all samples and temperatures. The oscillatory trend was fitted by a simple empirical form, $\Delta J^{mod}_{bw,cw}(q) = \sum_1^N D_i \cos(qR_i) \exp[-b_i q^2]$. After several trials, we set $N = 4$ and $b_1 = b_2 = b_3 \neq b_4$, leaving D_i and R_i as free parameters. We obtained a good fit with the advantage of getting analytical forms for both the contribution to the reciprocal form factor $\Delta B^{mod}_{bw,cw}(r)$ and the kinetic energy $\Delta T^{mod}_{e,cw}$.

Eventually, we obtained $\Delta B^{mod}_{bw,cw}(r)$ that is also represented in figure 2 (right panel) for bulk water and λ_2 samples at the different temperatures of the experiment. It is apparent that $\Delta B^{mod}_{bw,cw}(r)$ keeps different from zero over a range below 3 Å, that is a range of distances typical of the hydrogen atoms bonds. The overall spatial dependence is very similar, and similar also to bulk water, in all samples. There are two major peaks at about 1 Å and 2 Å, which can be attributed to covalent O-H bonds and *hydrogen bonds*. We find also the indication of a contraction of these bonds in all samples, with an average decrease of about 2 % for both peaks when the temperature decreases. Although $B(r)$ clearly contain information about the bond lengths, the procedure is not reliable enough to determine the variation of the bond contraction of different samples with temperature. Accordingly in the following analyses, we will rely on the experimental profiles to derive further quantitative information on the water bonding in the Nafion membrane and use the above numerical approach as an additional confirmation for such investigations. This approach revealed however more powerful for the evaluation of kinetics energy analysis, which involves integrals over the full momentum range.

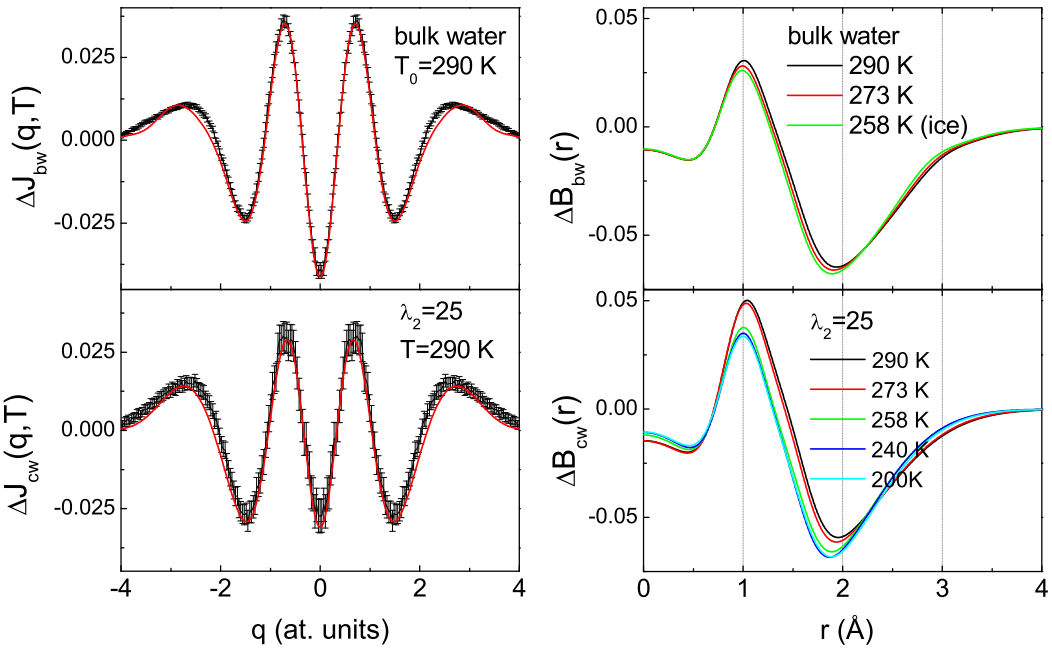

FIG. 2. Left: difference between experimental water CP and modeling with a linear combination of core and valence electron CP. Solid red lines are the fit to this difference with the analytical form described in the text. Top, bulk water $\Delta J_{bw}^{mod}(q,T_0)$; bottom : $\Delta J_{cw}^{mod}(q,T_0)$ for $\lambda_2 = 25$. Right: $\Delta B_{cw}^{mod}(r)$ for bulk water and λ_2 sample, at the various temperatures.

II. RESULTS

A. Hydration under vapor: water confined in the relaxed membrane

As previously emphasized, hydrating the membrane under water has a different effect than soaking it into water and structural changes of the membrane itself occur during water hydration. The polymer backbone is then expected to have the same conformation, so the same CP in both dry and room hydration, not at higher hydration. We consider in this section the polymer at the lowest hydration level, $\lambda_1 = 13$.

Room temperature. We first consider the Compton data collected at the reference room temperature $T_0 = 290$ K, obtained with the sample in equilibrium with ambient atmosphere at room temperature. Accordingly, the data here collected could be analyzed at a good approximation directly subtracting the dry matrix from the hydrated sample, which reasonably amounts to obtain the CP of confined water, that is $J_{cw}(q,T_0) = J^1(q,T_0) - J_{dm}(q,T_0)$. We emphasize that the so-called dry state, because of its experimen-

tal preparation, still contains $1-2$ remaining water molecule directly surrounding the SO_3^- groups,[24]. Therefore, after dry matrix subtraction, these specific water molecules do not contribute to $J_{cw}(q,T_0)$.

$J_{cw}(q,T_0)$ can be compared to the bulk water profile $J_{bw}(q,T_0)$ and figure 3 shows the difference between confined and bulk water profiles, i.e. $\Delta J_w(q,T_0) = J_{cw}(q,T_0) - J_{bw}(q,T_0)$.

As apparent in figure 3, $\Delta J_w(q=0,T_0)$ is negative: since a more peaked distribution in the q-space means a broader electron density in the real space, the negative values shows that the average electron distribution in confined water is more localized than in the bulk system. This indicates an overall contraction of the water molecule and/or the hydrogen bond network, associated to a higher total electronic kinetic energy under confinement (see section II C). Structural distortions in water can arise from different degree of freedom including angles and bonds, all giving rise to different CP variations as shown in the calculations by Hakala et al.[25]. Among the possible conformational changes, we consider only the one giving an oscillation with a minimum at ~ 1.4 a.u., as observed in our system, which is the contraction of the OH distance. This effect is reported in the figure 3, with a scaling factor of 7.0 in order to obtain the same amplitude as the experimental data. If we consider that the amplitude of CP difference is proportional to the contraction of the OH distance, then we extrapolate a contraction of ~ 0.09 Å for water confined in Nafion at room hydration. This simplified model will be further discussed in the III part.

Those measurements need to be compared with the results by Reiter et al.[26], who performed a very close study (same technique, same sample). Both difference profiles have the same sign, although the amplitude measured in reference[26] is about ten times larger. This may be the result of a different normalization of data and background signals. To define the effect of the different procedures, we calculated the CP of Nafion and water using the atomic data obtained by the Hartree-Fock approximation to roughly simulate the normalization approach of Ref.[35]. It is seen that, using a subtraction of the Nafion membrane contribution by imposing a negligible contribution of water when $q > 3$ au, introduces a slight reduction of the simulated confined water profile at low q so that the difference from the bulk water contribution appears enhanced. This effect is mainly due to the core (1s) electron contributions of different atoms present in nafion (C, O, F and S) and water (H and O). As a consequence, a different procedure in subtracting various CPs can enhance the confinement effect. Accordingly, the similar effect found in Ref.[26] on an other compound based on the

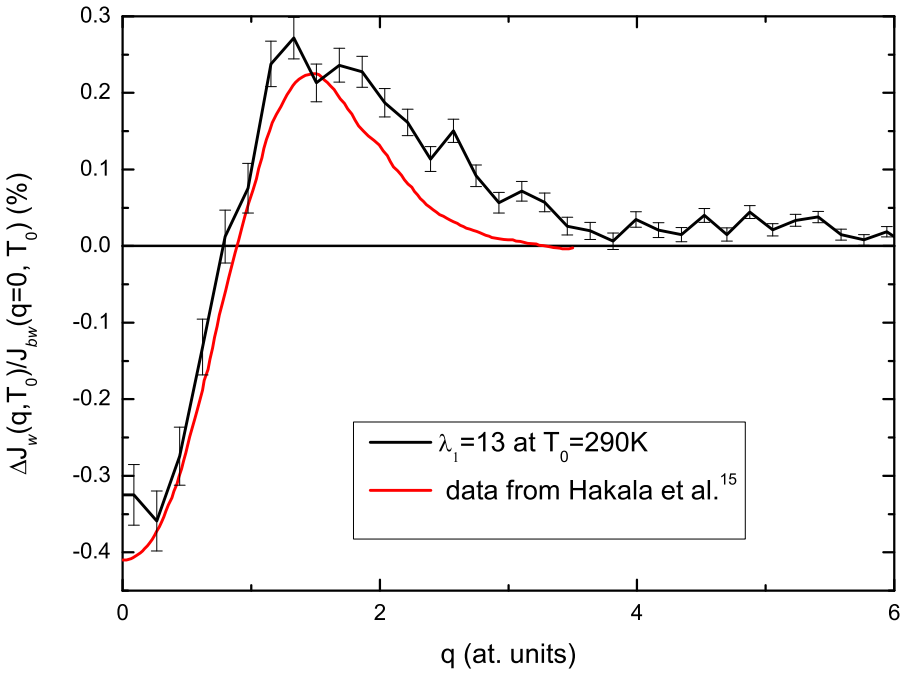

FIG. 3. Ratio between the CP difference at T_0 for the sample λ_1 and the CP of confined water, i.e. $\Delta J_w(q,T_0)/J_{bw}(q=0,T_0)$. The profile expected for an OH bond contraction equal to 0.09 Å, scaled from the figure 3 of reference[25] is also represented.

same elements as Nafion can be expected to produce the same result. Considering the small effect one is looking for in all cases, we believe that the surprisingly large effect observed in the study of Ref.[35], which is similarly observed in very different systems[27], deserved further investigations. Indeed, apart from the above discussed data analysis which needs further consideration, the slightly different preparation procedure of the dry membrane in the two experiments can produce an unequal number of *residual* water molecules per sulfonic group. These molecules could have a specific structure, thus affecting the observed change of the CP of confined water, as observed in the experiments. Here, we propose an alternative analysis of the present experimental data.

Temperature dependence. The differences between the CPs of *cw* measured at the temperature T and bulk water at $T_0 = 290$ K, $\Delta J_w(q,T) = J_{cw}(q,T) - J_{bw}(q,T_0)$, are shown in figure 4. The profiles were normalized by $J_w(0,T)$ to emphasize their similar, temperature-independent, shape.

The inset in figure 4 shows that with decreasing temperature, the absolute value of $\Delta J_w(q=0,T)/J_{bw}(q=0,T_0)$ increases. The temperature trend shown in the inset can

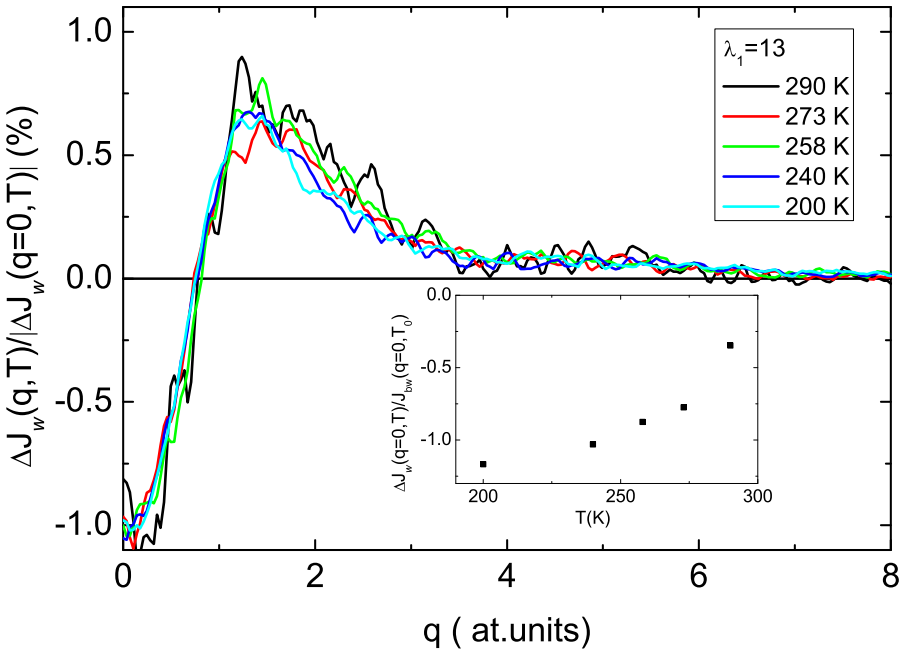

FIG. 4. Difference $\Delta J_w(q,T)$ between confined water CP at temperature T and the bulk water CP at T_0, after normalization by $\mid \Delta J_w(q=0,T) \mid$. The inset shows the temperature dependence of $\Delta J_w(q=0,T)/J_{bw}(q=0,T_0)$.

be compared with what is observed in bulk water when varying temperature. Hakala et al.[14] investigated bulk water over the temperature range 274 K - 364 K, and observed that the maximum variation of CP differences reaches about 0.2 %. For a similar 90 degrees temperature jump, namely from 200 K to 290 K, we measured a variation of $\sim$ 0.8 %. This comparison indicates that the water confined in the sample λ_1 undergoes a stronger contraction of the water bond length on decreasing temperature than bulk water.

Similarly, the integral of the absolute value of the CP difference varies from 6 to 14 % between 200 and 290 K, to be compared to a variation from 2 to 4.5 % in bulk water between 274 and 364 K respectively (see[14], fig 1.). This confirms that confined water is subjected to larger structural modifications upon temperature variation than bulk water.

B. Hydration in liquid boiling water: CP variation due to membrane swelling.

The samples at higher hydration, namely λ_2, λ_3 and λ_4, were obtained by boiling the membrane into water. The highest hydration level (nominal hydration level $\lambda_4 = 65$) was measured on a sample made of Nafion layers directly taken out of water, while the samples

at the two lower hydration levels, namely $\lambda_3 = 49$ and $\lambda_2 = 33$ (nominal hydrations), were obtained by pumping on the λ_4 sample.

As expected, the direct subtraction of the dry matrix spectrum, as in the case of the λ_1 sample, returned nonphysical results. Indeed, as pointed out in earlier studies[7,19,20], the structure of the matrix itself changes upon hydration because of the strong swelling process, which causes the creation of small volumes where additional water locates. Although definitive conclusions about the structural modifications upon swelling have not been achieved, the increased hydration of these samples is no more confined to sulfonic groups only. The use of the λ_2 sample as a reference for the matrix of the other two higher hydration samples also provides unreliable results, suggesting that the matrix changes *continuously* upon increasing hydration in addition to undergoing very slow relaxations[28].

In the following analysis, we make the assumption that the CP variations due to the confined water with respect to bulk water are identical to those measured in the vapor-hydrated sample, differing only by a scaling factor. In other words, we assume that the structural deformation are identical, only their amplitude varies with hydration. Therefore, the measured CP of each λ_i ($i > 1$) sample, $J^i(q, T_0)$, was linearly fitted with the sum of three components, $J^i_{fit}(q, T_0)$, namely the dry matrix, the bulk water and $\Delta J_w(q, T_0)$ as follows:

$$J^i_{fit}(q, T_0) = w^i_{dm}\ J_{dm}(q, T_0) + w^i_{bw}\ J_{bw}(q, T_0) + w^i_{\Delta}\ \Delta J_w(q, T_0) + b \tag{7}$$

where w^i_{dm}, w^i_{bw} and w^i_{Δ} are the weights of the three components. The weight w^i_{Δ} is therefore the amplitude of the structural variations of water confined in sample i with respect to sample 1. A constant level of background b was added for a better fitting of the data and to compensate possible very small systematic errors in the data reduction (e.g. background subtraction, multiple scattering), which, indeed, are visible on the CP wings at high q (see figure 1). This background level was found to be very low in any case. The weight w^i_{dm} of dry matrix subtraction was left free because the different measurements were carried out on two different samples (see Samples section), but its variation did not exceed $\sim 5\%$. By a proper normalization to the total number of electrons in the hydrated samples, given by the contribution from Nafion and hydration water for each sample, the ratio w^i_{bw}/w^i_{dm} provides an estimate of the sample hydration, (given in table I) and w^i_{Δ} provides the amplitude of the CP of confined water for each sample ($i > 1$).

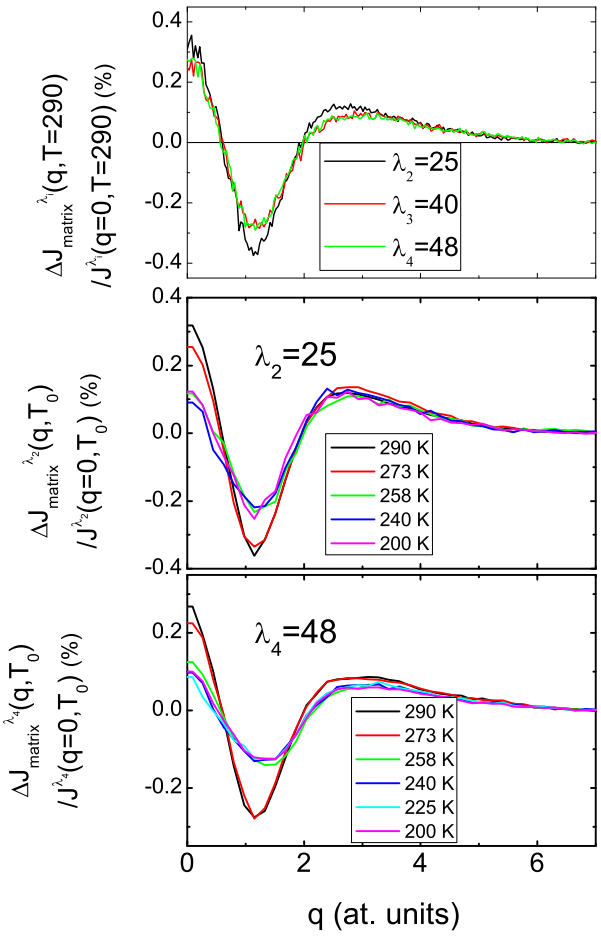

FIG. 5. Residual CP $\Delta J^i_{matrix}(q,T_0)/J^i(q=0,T_0)$ obtained as described in the text for the three samples λ_2, λ_3, λ_4. Note that this contribution is 0 for the sample 1. Top: all samples at room temperature $T_0 = 290$ K. Middle: sample λ_2 at the different temperatures. Bottom : same for sample λ_4.

We obtain this way the following results:

(i) the total hydration turns out to be in fair agreement with the nominal hydration obtained by sample weighting (see table I);

(ii) the residual contribution, namely $\Delta J^i_{matrix}(q,T_0) = J^i(q,T_0) - J^i_{fit}(q,T_0)$, is assigned to the deformed matrix and discussed below;

(iii) the ratio w^i_Δ/λ_i as a function of the nominal hydration value λ_i, giving the temperature dependence of the water contribution also discussed below.

Matrix contribution As previously discussed, the Nafion matrix of samples $\lambda_{2,3,4}$ is expected to be distorted with respect to the λ_1. Indeed, the residual contribution to the

CP is similar in all the samples and can be therefore assigned to the structural change in the matrix. These contributions are plotted in the figure 5, at room temperature on the top graph. We do not consider meaningful the small difference of $\Delta J^2_{matrix}(q, T_0)$ with the two others as it is within the range of possible systematic errors. All the $\Delta J^i_{matrix}(q = 0, T_0)$ are positive, supporting the picture of a more localized distribution in the reciprocal space or, alternatively, more delocalized in real space. This is consistent with the stretching of the polymer upon swelling when soaked into water.

We then observe a decrease of this matrix contribution as the temperature decreases, or said differently, the hydrated polymer structure is closer to the dry polymer at lower temperature (middle and bottom panels, 5). Furthermore, the evolution of the matrix with temperature is independent of hydration, since the profiles are similar for both λ_2 and λ_4. In particular, the largest variation is observed between 273 K and 258 K, that is over a temperature range where water desorbs out of the membrane, as shown in previous studies[29,30]. A simultaneous record of the diffraction pattern indeed confirms that ice starts forming in both samples when decreasing the temperature below 258 K.

Investigations of polymer conformational variations by Compton spectroscopy was previously addressed by Juurinen et al.[31] on hydrated PNIPAM polymer across its folding transition. The differences in CP observed between the folded or unfolded states of the polymer are very similar in shape and amplitude to the contribution plotted in figure 5 arising from the Nafion polymer deformation. In the PNIPAM study, the profile differences are assigned to the formation/breaking of hydrogen bond, together with covalent bond length variations either of the polymer and of the surrounding water. The situation of Nafion hydration in bulk/hot water, when water penetrates the interstices of the polymer backbone affecting the electronic distribution of the polymer is therefore very similar, from the electronic distribution point of view, to the PNIPAM folding-unfolding reversible phase transition at 37^oC.

Water contribution The figure 6 shows the amplitude of the confined water component (w^i_Δ), normalized to the hydration value, for each sample. We first emphasize that the values are much lower than 1, meaning that the difference between confined and bulk water in samples λ_2, λ_3 and λ_4, which have been hydrated in boiling water, are smaller than in the sample λ_1 obtained at room hydration. This observation is consistent with a profile of confined water closer to that of bulk water when the hydration is high. For the three *boiled*

samples, however, we do not observe, within the error bars, any further trend of profile variation.

We should note that, although water desorbs out of the membrane, the quantity of water contained in the measurement volume is constant, either liquid inside the matrix or as ice outside of the membrane. The total CP difference therefore includes both the differences between confined and bulk water, and those between ice and bulk water. The sample hydration, given by the ratio w^i_{bw}/w^i_{dm}, was therefore kept constant for all the temperature values and equal to that obtained by the T_0 fit. A distinction of water and ice in the CP may have been performed. However, looking at the CPs of water at 298 K and ice at 223 K reported in reference[32], it appears that the difference between the CPs of confined and bulk water is quite similar to the difference between the CPs of ice and liquid water. A more sophisticated fitting based on the confined water and ice difference profiles was therefore unsuccessful.

The lower panels of the figure 6 show the same quantity, normalized weight w^i_Δ/λ_i, as a function of temperature. These figures, as it was the case of $\Delta B_{cw}(r)$ in Fig. 2, reveal the presence of two different temperature trends, that will be discussed in the III section.

C. Interaction between water and membrane: kinetic energy

A comparison of kinetic energies amounts to comparing the binding energies, which, when applied to the present system, enables to infer the change in the binding energy as a function of both hydration and temperature.

T_e calculated for bulk water from CP integration according to equation 6 gives a value close to the one experimentally measured for the water molecule[33], giving a credit to the results obtained from the difference of two CPs. We then first analyzed T_e related to the CPs of figure 3 by directly integrating the experimental data up to 8.0 a.u., without subtracting the core electron contribution since only CPs differences are addressed. The temperature dependence of the ratio $\Delta T_e/T_e^{bw}(T_0)$, where $\Delta T_e = T_e^{cw}(T) - T_e^{bw}(T_0)$ is the excess of kinetic energy (at T) of confined water with respect to bulk water (at T_0), was calculated for $\lambda_1 = 13$ sample and shown in figure 7 (inset of left panel). As we commented before, an accurate and absolute detemination of the kinetic energy is rather difficult but, within the limit of the present measurements and analysis performed on various samples, we find that the kinetic

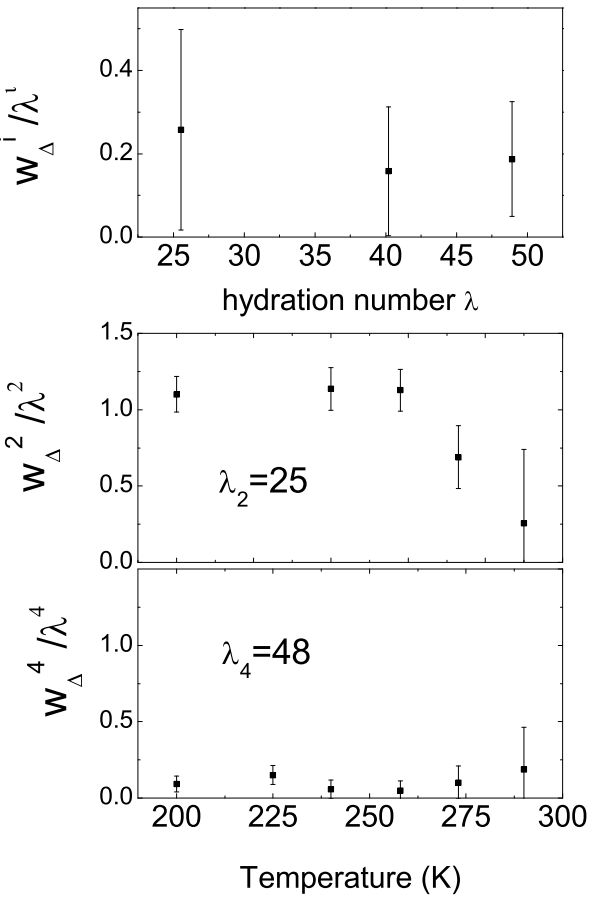

FIG. 6. Normalized weight w^i_Δ/λ_i of the confined water contribution for the higher hydration. Top: all samples at room temperature. Middle, bottom: temperature dependence for the λ_2 and λ_4 samples. Note the different trend of this ratio in the two samples.

energy of confined water of the λ_1 sample exceeds that of bulk water by a few percent at low temperature. This result support the presence of a strong interaction between water and the membrane, which can be assigned to the formation of a different water structure. A slow and continuous decreasing trend of the energy is observed in going from 200 K to 250 K with a faster rate from 250 K up to 290 K, indicating a progressive reduction of the water-membrane interaction with water becoming more similar to its bulk form. A similar behavior is seen in the inset of Fig. 4 for what concerns $\Delta J_w(q=0,T)/J_{bw}(q=0,T_0)$, which is a measure of the structural change. Therefore, considering that in the λ_1 sample there is no indication of water freezing in the whole temperature range we explored, an evident structural change of confined water is present. This result could be related to the general behavior of supercooled water in different confined environments.

The kinetic energy differences for the higher hydration samples, avoiding contributions from the membrane itself, can be directly deduced from the energy of the λ_1 sample modulated by the scaling factor w^i_Δ plotted in the figure 6 as a function of hydration and temperature. The temperature dependence can, however, be better examined when looking at the kinetic energy with respect to the lowest temperature, 200 K: $(T^{cw}_e(T) - T^{cw}_e(200))/T^{bw}_e(T_0)$. Similarly to what observed in figure 6, two different trends are observed for low and high hydration, as represented in the figure 7 (left).

As observed in the section I C, the kinetic energy calculation becomes difficult by error cumulation effects over the high momentum region. In order to confirm this unexpected behaviour, we therefore use the alternative analysis by directly integrating $\Delta J^{mod}(q,T)$ (still according to equation 6), at the various temperatures for the λ_1, λ_2, λ_4 samples and bulk water.

The corresponding quantities, $(T^{mod}_e(T) - T^{mod}_e(200))/T_{e,mol}$, are shown in the right part of the figure 7. The reliability of the observed trends is supported by the similarity of the results applying the two computation methods. The higher hydration sample λ_4 shows a trend similar to bulk water, as can be expected for interstitial water. Differently, the λ_1 and λ_2 samples show a similar temperature behavior with a strong decrease of kinetic energy upon increasing temperature above $\sim 250K$, a behavior that we assign to the interaction with the surrounding sulfonic groups.

III. DISCUSSION ON THE WATER STRUCTURAL DISTORTIONS UPON CONFINEMENT

The quantitative interpretation or our data is based on several studies of Hakala et al.[14,25,34] on water. In particular, we propose a sizable contraction of the OH bond of ~ 0.09 Å for water confined in Nafion at room hydration. For higher hydration levels, this value scales by the w^i_Δ factor of figure 6. This leads to a contraction of about 0.02 Å. The bond contraction observed in this way is similar to that derived from the peaks of $\Delta B_{cw}(r)$. We emphasize however that this does not provide a picture of the electronic bond in real space. The picture of the OH bond length modification without other distortion is a simplification. However, it enables having a quantitative picture of the structural contraction under the form of a simply defined structural averaged parameter. A more accurate evaluation of the

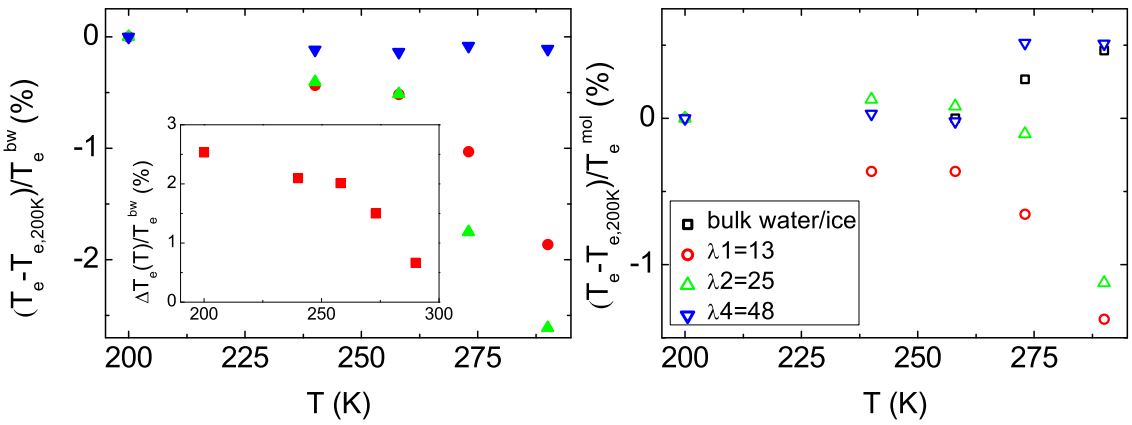

FIG. 7. Left: temperature dependence of the kinetic energy T_e for λ_1, λ_2, λ_4 samples; the kinetic energy changes with respect to the lowest temperature (T = 200 K) are divided by the bulk water energy T_e^{bw} at T_0. Insert: temperature dependence of the ratio $\Delta T_e(T)/T_e^{bw}(T) = (T_e^{cw}(T) - T_e^{bw}(T_0))/T_e^{bw}(T_0)$ determined for the λ_1 sample. Right: the same as left panel, but calculated from the integration of $\Delta J^{mod}(q,T)$, and normalized to the value experimentally measured for the single water molecule T_e^{mol} = 152.8752 Ryd.[33]

bond distortions could be obtained in performing the calculation for the different geometries, instead of assuming a linear scaling. Indeed, considering the temperature dependence, one could extrapolate that water confined in the Nafion membrane at 200 K, giving a four times larger difference in CP (see insert of fig. 4), would have a difference in OH bond length of about 0.36 Å, which is not reasonable. It is clear that other distortions, specially at low temperature, account for the CP differences.

Structural modification of ice under pressure presents a relevant comparison. The study of Bellin et al.[35]. which measures the CP variation in the different forms of ices under high pressure offers this possibility. The largest differences are observed between Ih and Ice VIII that is formed under 5 GPa of external load, leading to OH contraction of 0.07 Å (although 0.2 Å after correction by the oxygen disorder) and an increase in density from 0.92 g/cm^3 up to 1.5 g/cm^3. The measured amplitude at q=0 is $\Delta J(0) = 0.012$, $\Delta J(0)/J(0) \sim 0.4$ %, comparable or larger than our results.

The kinetic energy analysis demonstrate a higher energy for confined water with respect to bulk water. The energy difference increases upon cooling, although the energy of confined water is always compared to bulk water at room temperature, neglecting the bulk water en-

ergy evolution. Analyzing the temperature dependences highlights two regimes of hydration. A first strongly interacting regime is observed for λ_1=13, when water fills the cavities formed by the sulfonic groups, where interaction increases further upon cooling. The second regime is observed for λ_4=48, when water fills the interstices between the polymer fibers. The gain in kinetic energy is smaller, in agreement with the simple observation that water is more difficult to be kept inside the polymer at such high hydration. The λ_2=25 sample is found to be in between. Two different analysis lead to similar result. The second analysis however also takes into account the kinetic energy variations arising from the polymer, as only the dry matrix, that was proven to be different from the actual matrix for λ_2=25 and λ_4=48, was subtracted to the raw data. Since the differences in T_e extracted by the second methods are smaller that with the first ones, the difference between both methods may indicate that the energy variation for water and polymer are of opposite sign. This energy difference could explain the *interstitial* water desorption out of the membrane at subzero temperature.

CONCLUSION

We carried out a Compton spectroscopy study of hydrated Nafion membranes as a function of temperature and hydration, addressing several questions: (i) the structure of confined water and the distortion of hydrogen bond network and its temperature dependence; (ii) the interaction energy between water molecules and the membrane and (iii) the deformation of the polymer upon swelling at the molecular level.

The distortion of hydrogen bond network are interpreted in terms of an averaged OH bond contraction. Although this may be a simplified picture, it enables a quantitative description of the water structural modification that can be followed in different systems. We also identified two water populations. The water molecules strongly interacting with the ionic sulfonic groups undergo large structural modifications. We still emphasize that the number of affected molecules is large, 13 water molecules per sulfonic group, i.e. far more than the two bounded molecules. Water molecules filling the interstices of the polymer are less affected.

The energetics analysis provides an overall consistent picture of the water behavior in Nafion, in agreement with the previous CP analysis. Validated by two different analysis, we conclude that the water is energetically favored when penetrating into the membrane

with a transition regime around 250 K. This behavior seems to be a general feature of water in nano-confinement or close to (charged) surfaces[36]. For instance, at the much lower thermic energy level of atomic dynamics, hydration water structure has a basic role in the protein structure and dynamics[37], and has some relationship to functionality. Also, different disordered structures of protein hydration water appear to be present affecting the total water dynamics[38].

Eventually, we find that polymer deformation have a strong impact of the CP, similarly to what is observed in the folding-unfolding transition if PNIPAM. This could provide a powerful tool to follow polymeric systems reorganization such as proteins.

ACKNOWLEDGMENTS

We thank ESRF for beamtime allocation. The project was funded by the European Grant Agreement No 284522 - H2FC.

DATA AVAILABILITY

Raw data were generated at the ESRF large scale facility. Derived data supporting the findings of this study are available from the corresponding author upon reasonable request.

REFERENCES

[1]D. Demuth, M. Reuhl, M. Hopfenmüller, N. Karabas, S. Schoner, and M. Vogel, "Confinement effects on glass-forming aqueous dimethyl sulfoxide solutions," Molecules **25** (2020), 10.3390/molecules25184127.

[2]K. A. Mauritz and R. B. Moore, "State of understanding of Nafion," Chemical Reviews (2004).

[3]A.-C. Dupuis, "Proton exchange membranes for fuel cells operated at medium temperatures: Materials and experimental techniques," Progress in Materials Science **56**, 289–327 (2011).

[4]T. D. Gierke, G. E. Munn, and F. C. Wilson, "The morphology in nafion perfluorinated membrane products, as determined by wide- and small-angle x-ray studies," Journal of Polymer Science: Polymer Physics Edition **19**, 1687–1704 (1981).

[5]K. Schmidt-Rohr and Q. Chen, "Parallel cylindrical water nanochannels in Nafion fuel-cell membranes," Nature Materials **7**, 75–83 (2008).

[6]K. Kreuer and G. Portale, "A critical revision of the nano-morphology of proton conducting ionomers and polyelectrolytes for fuel cell applications," Advanced Functional Materials **23**, 5390–5397 (2013).

[7]A. Kusoglu, S. Savagatrup, K. T. Clark, and A. Z. Weber, "Role of Mechanical Factors in Controlling the Structure-Function Relationship of PFSA Ionomers," Macromolecules (2012).

[8]A. Kusoglu, M. a. Modestino, A. Hexemer, R. a. Segalman, and A. Z. Weber, "Subsecond Morphological Changes in Nafion during Water Uptake Detected by Small-Angle X-ray Scattering," ACS Macro Letters **1**, 33–36 (2012).

[9]F. Sacchetti, A. Orecchini, A. Cunsolo, F. Formisano, and C. Petrillo, "Coherent neutron scattering study of confined water in nafion," Phys. Rev. B **80**, 024306 (2009).

[10]S. Cerveny, F. Mallamace, J. Swenson, M. Vogel, and L. Xu, "Confined Water as Model of Supercooled Water," Chemical Reviews **116**, 7608–7625 (2016).

[11]A. W. Knight, N. G. Kalugin, E. Coker, and A. G. Ilgen, "Water properties under nano-scale confinement," Scientific Reports **9**, 1–12 (2019).

[12]A. K. Soper, "Density minimum in supercooled confined water," Proceedings of the National Academy of Sciences of the United States of America **108**, 2011 (2011).

[13]M. J. Cooper, "Compton-scattering and electron momentum distribution," Reports on Progress in Physics **48**, 415–481 (1985).

[14]M. Hakala, K. Nygård, S. Manninen, S. Huotari, T. Buslaps, A. Nilsson, L. G. Pettersson, and K. Hämäläinen, "Correlation of hydrogen bond lengths and angles in liquid water based on Compton scattering," Journal of Chemical Physics **125** (2006), 10.1063/1.2273627.

[15]T. A. Zawodzinski, "Water Uptake by and Transport Through Nafion® 117 Membranes," Journal of The Electrochemical Society **140**, 1041 (1993).

[16]B. MacMillan, A. R. Sharp, and R. L. Armstrong, "An n.m.r. investigation of the dynamical characteristics of water absorbed in Nafion," Polymer **40**, 2471–2480 (1999).

[17]D. Rivin, C. Kendrick, P. Gibson, and N. Schneider, "Solubility and transport behavior of water and alcohols in Nafion™," Polymer **42**, 623–635 (2001).

[18]N. J. Bunce, S. J. Sondheimer, and C. a. Fyfe, "Proton NMR method for the quantitative determination of the water content of the polymeric fluorosulfonic acid Nafion-H,"

Macromolecules **19**, 333–339 (1986).

[19]G. Gebel, "Structural evolution of water swollen perfluorosulfonated ionomers from dry membrane to solution," Polymer **41**, 5829–5838 (2000).

[20]R. Hammer, M. Schönhoff, and M. R. Hansen, "Comprehensive Picture of Water Dynamics in Nafion Membranes at Different Levels of Hydration," The Journal of Physical Chemistry B **123**, 8313–8324 (2019).

[21]R. Ribberfors, "Relationship of the relativistic compton cross section to the momentum distribution of bound electron states," Phys. Rev. B **12**, 2067–2074 (1975).

[22]P. Fajardo, V. Honkimäki, T. Buslaps, and P. Suortti, "Experimental validation of multiple scattering calculations with high energy x-ray photons," Nuclear Instruments and Methods in Physics Research Section B: Beam Interactions with Materials and Atoms **134**, 337 – 345 (1998).

[23]L. V. Azàroff, R. Kaplow, N. Kato, R. J. Weiss, A. J. C. Wilson, and R. A. Young, "X-ray diffraction," , 594–608 (1974).

[24]S. Dalla Bernardina, J.-b. Brubach, Q. Berrod, A. Guillermo, P. Judeinstein, P. Roy, and S. Lyonnard, "Mechanism of Ionization, Hydration, and Intermolecular H-Bonding in Proton Conducting Nanostructured Ionomers," The Journal of Physical Chemistry C **118**, 25468–25479 (2014).

[25]M. Hakala, K. Nygård, S. Manninen, L. G. M. Pettersson, and K. Hämäläinen, "Intra- and intermolecular effects in the Compton profile of water," Physical Review B - Condensed Matter and Materials Physics **73**, 1–9 (2006).

[26]G. F. Reiter, A. Deb, Y. Sakurai, M. Itou, V. G. Krishnan, and S. J. Paddison, "Anomalous ground state of the electrons in nanoconfined water," Physical Review Letters **111**, 1–5 (2013).

[27]G. F. Reiter, A. Deb, Y. Sakurai, M. Itou, and A. I. Kolesnikov, "Quantum Coherence and Temperature Dependence of the Anomalous State of Nanoconfined Water in Carbon Nanotubes," Journal of Physical Chemistry Letters **7**, 4433–4437 (2016).

[28]M. Fumagalli, S. Lyonnard, G. Prajapati, Q. Berrod, L. Porcar, A. Guillermo, and G. Gebel, "Fast Water Diffusion and Long-Term Polymer Reorganization during Nafion Membrane Hydration Evidenced by Time-Resolved Small-Angle Neutron Scattering," Journal of Physical Chemistry B **119**, 7068–7076 (2015).

[29]M. Plazanet, P. Bartolini, R. Torre, C. Petrillo, and F. Sacchetti, "Structure and acoustic properties of hydrated nafion membranes," The Journal of Physical Chemistry. B **113**, 10121–7 (2009).

[30]M. Plazanet, F. Sacchetti, C. Petrillo, B. Demé, P. Bartolini, and R. Torre, "Water in a polymeric electrolyte membrane : Sorption / desorption and freezing phenomena," Journal of Membrane Science **453**, 419–424 (2014).

[31]I. Juurinen, S. Galambosi, A. G. Anghelescu-Hakala, J. Koskelo, V. Honkimäki, K. Hämäläinen, S. Huotari, and M. Hakala, "Molecular-level changes of aqueous poly(N -isopropylacrylamide) in phase transition," Journal of Physical Chemistry B **118**, 5518–5523 (2014).

[32]K. Nygård, M. Hakala, S. Manninen, A. Andrejczuk, M. Itou, Y. Sakurai, L. G. Pettersson, and K. Hämäläinen, "Compton scattering study of water versus ice Ih: Intra- and intermolecular structure," Physical Review E - Statistical, Nonlinear, and Soft Matter Physics **74**, 1–5 (2006).

[33]D. Feller, C. M. Boyle, and E. R. Davidson, "One-electron properties of several small molecules using near hartree–fock limit basis sets," The Journal of Chemical Physics **86**, 3424–3440 (1987).

[34]M. Hakala, S. Huotari, K. Hämäläinen, S. Manninen, P. Wernet, A. Nilsson, and L. G. Pettersson, "Compton profiles for water and mixed water-neon clusters: A measure of coordination," Physical Review B - Condensed Matter and Materials Physics **70**, 1–8 (2004).

[35]C. Bellin, B. Barbiellini, S. Klotz, T. Buslaps, G. Rousse, T. Strässle, and A. Shukla, "Oxygen disorder in ice probed by x-ray Compton scattering," Physical Review B - Condensed Matter and Materials Physics **83**, 1–5 (2011).

[36]G. F. Reiter, A. I. Kolesnikov, S. J. Paddison, P. M. Platzman, A. P. Moravsky, M. A. Adams, and J. Mayers, "Evidence for an anomalous quantum state of protons in nanoconfined water," Physical Review B - Condensed Matter and Materials Physics **85**, 1–5 (2012).

[37]M.-C. Bellissent-Funel, A. Hassanali, M. Havenith, R. Henchman, P. Pohl, F. Sterpone, D. van der Spoel, Y. Xu, and A. E. Garcia, "Confinement effects on glass-forming aqueous dimethyl sulfoxide solutions," Chem. Rev. **116**, 7673–7697 (2016).

[38]A. Paciaroni, A. Orecchini, E. Cornicchi, M. Marconi, C. Petrillo, M. Haertlein, M. Moulin, H. Schober, M. Tarek, and F. Sacchetti, "Fingerprints of amorphous icelike behavior in

the vibrational density of states of protein hydration water," Phys. Rev. Lett. **101**, 148104 (2008).